Homogeneous Free Radical Polymerizations in Supercritical Carbon Dioxide: 2. Thermal Decomposition of 2,2′-Azobis(isobutyronitrile)

Zhibin Guan, J. R. Combes, Y. Z. Menceloglu, and J. M. DeSimone*

CB# 3290, Venable and Kenan Laboratories, Department of Chemistry, University of North Carolina at Chapel Hill, Chapel Hill, North Carolina 27599-3290

Received November 25, 1992; Revised Manuscript Received February 15, 1993

ABSTRACT: The thermal decomposition of 2,2′-azobis(isobutyronitrile) (AIBN) in supercritical CO_2 was investigated by using UV/vis spectroscopic methods. The solvent strength of CO_2 was characterized using solvatochromic measurements with 9-(α-(perfluoroheptyl)-β,β-dicyanovinyl)julolidine. The measured solvent strength of supercritical CO_2 aided in the interpretation of the observed effects of density on the decomposition kinetics. Analysis of the decomposition products indicated that supercritical CO_2 is an acceptable medium to conduct free radical reactions. The decomposition rate and initiation efficiency of AIBN in supercritical CO_2 as a function of pressure and temperature were determined and modeled using Kirkwood solution theory. The decomposition rate of AIBN in supercritical CO_2 was found to be considerably lower than that observed in benzene at the same temperatures and pressures due to the lower dielectric constant of CO_2 relative to benzene. The initiation efficiency of AIBN in supercritical CO_2 was shown to be ca. 1.5 times higher than that measured in benzene and was found to be invariant with pressure.

Introduction

Recently, we reported the first successful homogeneous free radical polymerization in an inert supercritical fluid (SCF).[1] We showed that a series of highly fluorinated acrylic monomers could be successfully polymerized to form a variety of fluorinated homopolymers and copolymers (with nonfluorinated comonomers) using homogeneous free radical polymerization methods in supercritical CO_2. Generally, the amorphous polymers that contain a large fraction (>80 wt %) of the fluorinated acrylic monomers are insoluble in most organic solvents except some chlorofluorocarbons (CFCs). CFCs have been identified as one of the main causes of the depletion of the atmospheric ozone layer.[2] The synthesis of fluoropolymers in CO_2 not only offers an environmentally sound solvent choice but offers much more in the context of being able to do certain chemical transformations in one phase (*allows for the synthesis of copolymers and functional polymers*) having an inherently low solution viscosity (*no Tromsdorff effects or autoacceleration at high conversions*) under inert conditions (*no detectable chain transfer to solvent*). Moreover, because of the significant compressibility of SCFs, important physical properties—density, dielectric constant, solubility parameter, and transport properties—can be easily controlled and systematically varied, providing a unique method to investigate solvent effects on chemical reactions to influence reaction rates and selectivities.[3]

There are a number of applications in which the processing of polymers in supercritical fluid phases is useful, e.g., the extraction of low molecular weight contaminants and the fractionation of polymers or copolymers by molecular weight and/or composition,[4–11] and there is a high potential for the use of SCFs as reaction solvents.[12] However, the use of chemically inert SCFs as polymerization media has remained a relatively unexplored area. Ehrlich and co-workers realized early on that the high-pressure, high-temperature process for the polymerization of ethylene was actually a supercritical fluid process where high molar mass polyethylene is soluble in supercritical ethylene monomer.[13,14] In this particular case, the supercritical fluid solvent is also the reactant and the polymerization was usually done at pressures and temperatures that far exceed the critical pressure and temperature of ethylene. For the few reported polymerizations using a SCF as an inert solvent, the polymers formed were characterized by low yields and the polymerization systems became heterogeneous early on at low conversions.[15–18] Hence, detailed mechanistic investigations of homogeneous polymerizations in inert SCFs are scarce.

Our aim is to thoroughly investigate the kinetics of initiation, propagation, and termination steps for homogeneous free radical polymerizations in supercritical CO_2 as a function of pressure and temperature. The elevation of pressure for traditional types of heterogeneous and homogeneous polymerizations generally influences the course of events by (i) increasing the concentration of gaseous monomers (such as vinyl chloride and vinylidene fluoride); (ii) affecting the individual rate constants for initiation, propagation, termination, chain transfer, etc.; and (iii) affecting the equilibrium constant for the polymerization. Increasing pressure usually results in an increase in the polymerization rate and an increase in the molar mass.[19] The quantitative effect of pressure (at constant temperature) on an individual rate constant is given by

$$\left(\frac{\delta \ln k}{\delta P}\right)_T = \frac{-\Delta V^{\ddagger}}{RT} \tag{1}$$

where $\Delta V^{\ddagger}$ is the activation volume and k is the reaction rate constant (expressed in pressure-independent concentration units). If a transition state approach is applicable to the kinetics, $\Delta V^{\ddagger}$ is the change in volume in going from the reactants to the transition state.[20] For a propagation reaction, $\Delta V^{\ddagger}_p$ is generally negative, and therefore increasing pressure increases the polymerization rate. However, the activation volume for initiation via thermal decomposition of a free radical initiator, $\Delta V^{\ddagger}_d$, is normally positive.[21] Herein, we report on our investigations on the thermally-induced decomposition of 2,2′-azobis(isobutyronitrile) (AIBN), a commonly used free radical initiator, in supercritical CO_2.

The mechanism for the thermal decomposition of AIBN is generally accepted[22–25] to be a homolytic scission

* Author to whom correspondence should be addressed.

0024-9297/93/2226-2663$04.00/0

Scheme I. Mechanism of Thermal Decomposition of AIBN

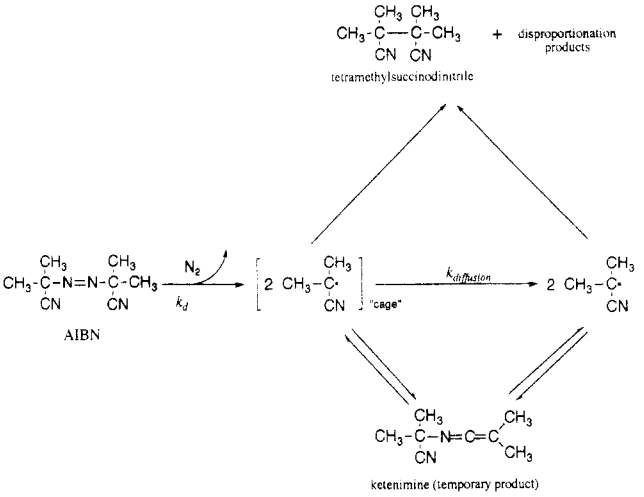

according to Scheme I. According to Hammond et al.,[26] the primary geminate radicals formed during the thermal decomposition of AIBN are formed in solvent "cages". These radicals will either diffuse out of the cage or form adducts inside the cage ("cage effect"). The fraction of the radicals which can diffuse out of the cage and therefore can initiate a polymerization is termed as the initiation efficiency, f, which can be determined by using a radical scavenger. In this study the major products of AIBN decomposition in CO_2 were analyzed and compared with those in tetrahydrofuran (THF). The decomposition rates and initiation efficiency in supercritical CO_2 at various pressures and temperatures were measured for AIBN.

The solvent strength of supercritical CO_2, an important variable to consider for polymerization reactions, has often been characterized with the aid of solvatochromic indicators.[27,28] The wavelength of maximum absorbance (or λ_{max}) for a dye molecule is a valuable indicator as to the degree to which the dye's excited state is stabilized by the surrounding solvent (or cosolvent) molecules. Herein, a solvent polarity scale based on the absorption of 9-(α-(perfluoroheptyl)-β,β-dicyanovinyl)julolidine[29]

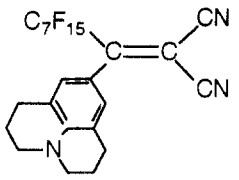

was used to characterize the solvent strength of supercritical CO_2 by observing the shift in λ_{max} with pressure. The λ_{max} results were converted to a normalized transition energy scale, and spectral polarity index values, P_s, were calculated as reported previously.[29,30] This particular solvent polarity scale is normalized to perfluorohexane (P_s = 0) and dimethyl sulfoxide (P_s = 10). These data were used to aid in the understanding of the temperature and pressure effects on the AIBN decomposition kinetics.

Experimental Section

Materials. Carbon dioxide (Matheson, 99.99%) was purified by passing through two columns filled with 4-Å molecular sieves and reduced copper oxide catalyst (BASF R3-11) to remove water and oxygen, respectively. AIBN (Eastman Kodak) was recrystallized twice from methanol. Galvinoxyl was purchased from Aldrich and used as received. Benzene (EM Science, GR) was refluxed over CaH_2 under argon and fractionally distilled. THF (Fisher Certified Grade) was refluxed over sodium/benzophenone and distilled under an argon atmosphere. 9-(α-(Perfluoroheptyl)-β,β-dicyanovinyl)julolidine was provided courtesy of Professor W. J. Middleton of Ursinus College and was used as received. Methanol (Mallinckrodt, HPLC grade) and hexane (EM Science, ACS grade) were used as received.

Solvatochromic Studies. The UV–visible absorption spectra of 9-(α-(perfluoroheptyl)-β,β-dicyanovinyl)julolidine in supercritical CO_2 were recorded on a Perkin-Elmer Lambda 6 spectrophotometer which was interfaced to an IBM PS/2 Model 50 computer running Perkin-Elmer Data Manager software. A high-pressure spectroscopic cell fitted with sapphire windows[30] was used for all the UV spectroscopic studies. Temperature control was achieved with the aid of a Lauda K6 circulating bath. Pressures were generated with a high-pressure syringe pump (High Pressure Equipment Inc., Model 62-6-10) and monitored with a pressure transducer (Sensotec Model TVE and Model GM display). All spectral measurements were performed by placing an aliquot of 9-(α-(perfluoroheptyl)-β,β-dicyanovinyl)-julolidine dissolved in hexane into the high-pressure spectroscopic cell followed by evaporation of the hexane with an argon purge. The loading procedure has been previously described.[27,30] For experiments in which a liquid cosolvent was added, the liquid was added to the cell under an argon purge after the hexane was removed. The cell was then sealed, raised to the desired temperature, and finally raised to the desired pressure with addition of carbon dioxide, and spectra were recorded after the system reached equilibrium (ca. 40 min). The λ_{max} results were converted to spectral polarity index values, P_s, as reported previously.[29,30]

Analysis of AIBN Decomposition Products. The products resulting from the thermal decomposition of AIBN in supercritical CO_2 and THF were analyzed by using ^1H NMR (Bruker AC200 NMR), ^{13}C NMR (Bruker AC200 NMR), and FT-IR (Nicolet IR spectrometer).

Decomposition Rate of AIBN. The thermal decomposition rates of AIBN were measured at different temperatures and pressures. Pressure effects on the decomposition rate (k_d) of AIBN in supercritical CO_2 were investigated by measuring the decomposition rates at various pressures at constant temperature (59.4 °C). The temperature dependence of k_d was also investigated by measuring the thermal decomposition of AIBN at 59.4, 69.3, and 79.4 °C at constant density (ρ = 0.7352 g/mL). A typical experiment proceeded as follows: AIBN (20 mg) was placed into the 10-mL high-pressure view cell containing a micromagnetic stir bar. The cell was purged with argon for ca. 10 min and was filled with CO_2 to approximately 68 bar. The temperature was raised to 59.4 (±0.1) °C and the final desired pressure was achieved with the addition of more CO_2. As the temperature and pressure reached the desired values, UV spectra were collected once every 30 min. The decomposition studies of AIBN in benzene were also conducted in the same high-pressure cell at identical experimental conditions. The absorbance of AIBN was obtained after spectral subtraction of pure benzene. All UV spectra were recorded on a Perkin-Elmer Lambda 6 UV/vis spectrophotometer.

Initiation Efficiency of AIBN. AIBN (10 mg) and galvinoxyl (2 mg), a radical scavenger, were put into the high-pressure view cell, purged with argon and filled with CO_2 to ca. 68 bar. The cell was heated to the desired temperature (59.4 °C), and the pressure was increased to the desired value by addition of more CO_2. UV/vis spectra of galvinoxyl were collected once every 5 min, and the absorbance was plotted versus time.

Results and Discussion

Solvatochromic Characterization of Supercritical CO_2. The solvent strength of supercritical CO_2—as correlated by its spectral polarity index[29]—varies dramatically with fluid pressure as shown in Figure 1. The observed trend reflects the highly pressure-dependent nature of solvent density for supercritical fluids near the critical point. Addition of a polar cosolvent (methanol or THF) can increase the solvent polarity significantly. Figure 1 shows that the addition of 5 vol % THF to CO_2 increases the spectral polarity index, P_s, approximately

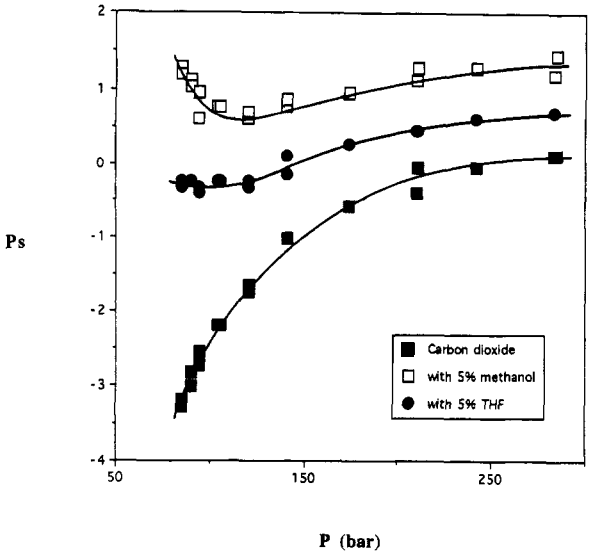

Figure 1. Solvatochromic studies of supercritical CO_2 at 59.4 (±0.5) °C.

0.5 units at high densities and almost 2 units at low densities. With addition of methanol as a cosolvent, an increase in the spectral polarity index is observed at lower pressures near the critical point despite the lower overall density of solvent. This increase can be attributed to the increasing mole fraction of methanol at lower pressure (the mass of methanol in the cell is constant with respect to pressure), thereby facilitating a greater average number of intermolecular interactions between methanol and the dye molecule relative to that between CO_2 and the dye and therefore the spectral polarity index approaches the value for pure methanol.[27] Another phenomenon contributing to this near-critical increase in P_s is a density fluctuation phenomenon commonly referred to as "clustering".[27,28,31] As fluids approach the critical point, the structure of solvent and cosolvent molecules surrounding a dye molecule may not necessarily be isotropic. Regions of locally augmented densities may be found in which the concentration of a cosolvent (i.e., methanol or THF) is higher than that expected based on the bulk composition of the fluid.

Product Analysis. The thermal decomposition products of AIBN in supercritical CO_2 were investigated with NMR and FTIR and compared to the products obtained in THF.[32] The ^1H NMR spectra of the AIBN decomposition mixtures in CO_2 and in THF show the major product to be the same, i.e., $Me_2(CN)C-CMe_2(CN)$. ^{13}C NMR spectra of the AIBN decomposition mixture from CO_2 did not contain any carbonyl resonance, which indicates the stability of the tertiary radical species and its resonant structures relative to a carboxy radical which would form if the tertiary radical added to CO_2. Time-resolved electron pair resonance[33] investigations are currently underway to evaluate if any transient carboxy radicals form at supercritical conditions and to measure their lifetimes. As reported by us previously,[1] structural analysis of fluoropolymers synthesized in supercritical carbon dioxide provides more evidence for the effective inertness of carbon dioxide toward these radical reactions. FTIR spectra of the decomposition mixtures in CO_2 and in THF were also similar.

Decomposition Rate. Figure 2 shows a typical series of UV/vis spectra of AIBN during thermal decomposition in CO_2 at 59.4 (±0.1) °C and 276 (±0.5) bar. The decreasing azo absorption at 347 nm corresponds to the loss of AIBN, and the increasing maximum at 290 nm corresponds to the formation of the temporary adduct, $Me_2(CN)$-

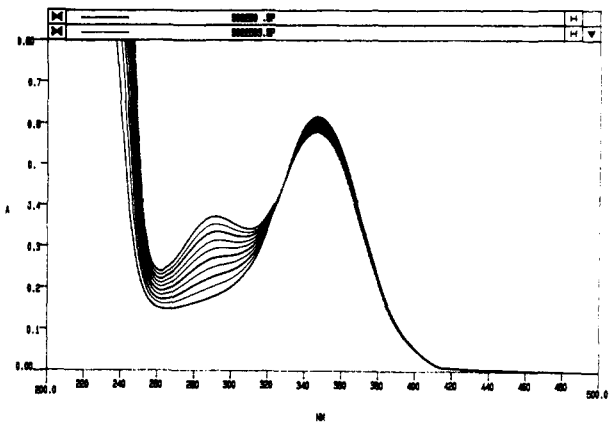

Figure 2. UV spectra for the thermal decomposition of AIBN in supercritical CO_2 at 59.4 (±0.1) °C and 276 (±0.5) bar; [AIBN] = 1.22×10^{-2} M. Spectra were collected once every 30 min.

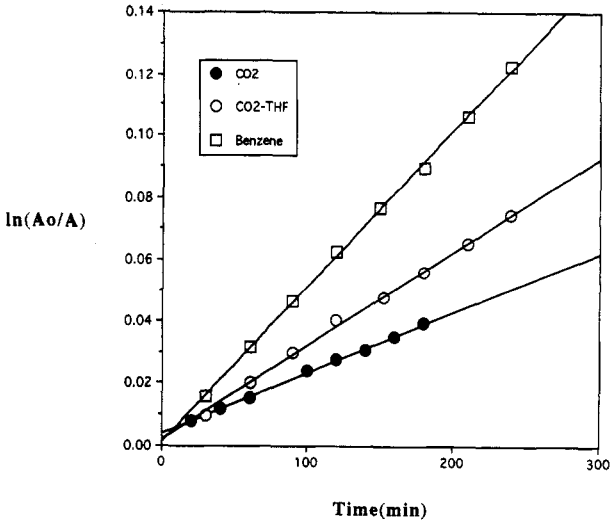

Figure 3. Graph of $\ln(A_0/A)$ (absorbance at 347 nm) versus time for AIBN thermal decomposition at 59.4 (±0.1) °C in benzene, CO_2 with 5 v/v % THF, and pure CO_2 at 207 (±0.5) bar.

$CN{=}C{=}CMe_2$, which forms from the recombination of primary radicals (see Scheme I).[22,34] The results are plotted in Figure 3 according to first-order kinetics. Figure 3 shows the decomposition of AIBN in supercritical CO_2 at 207 bar, in benzene at ambient pressure, and in a mixture of CO_2 and tetrahydrofuran (5 vol % THF) at 59.4 °C. The rate of AIBN decomposition in supercritical carbon dioxide ($k_d = 3.5 \times 10^{-6}$ s^{-1}) is ca. 2.5 times lower than that observed in benzene ($k_d = 8.4 \times 10^{-6}$ s^{-1}) at ambient pressure. However, the decomposition rate can be augmented by the addition of polar cosolvents as shown for the addition of only 5 vol % THF to CO_2.

The rate of thermal decomposition of AIBN in supercritical CO_2 was also measured at 69.3 and 79.4 (±0.1) °C at the same CO_2 density as at 59.4 °C and 207 bar (i.e., ρ = 0.735 g/mL). Following the same kinetic treatment (Figure 4), the rate constants at 70 °C (248 bar) and 80 °C (290 bar) were calculated to be 1.36×10^{-5} and 5.16×10^{-5} s^{-1}, respectively. The activation energy for the thermal decomposition of AIBN in supercritical CO_2 was calculated to be 134.6 kJ/mol from the Arrhenius plot. The activation energy measured in various organic solvents was reported to be in the range from 120 to 140 kJ/mol,[35] and therefore the activation energy determined in supercritical carbon dioxide is comparable to that found in conventional liquid solvents.

The variation of k_d as a function of pressure in CO_2 and in benzene is shown in Figure 5. The decomposition rates

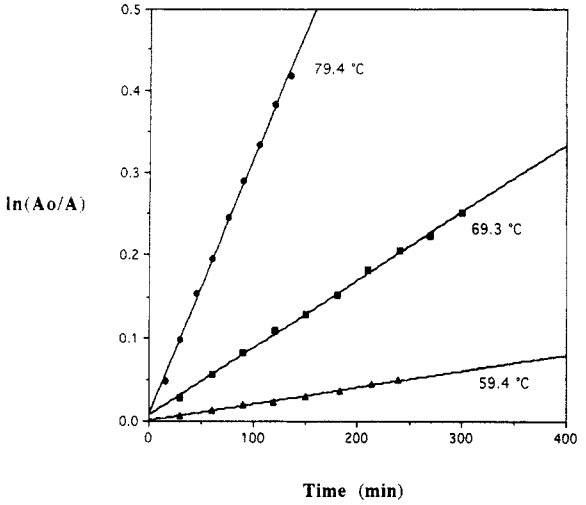

Figure 4. Temperature dependence of the thermal decomposition rate of AIBN in supercritical CO_2 at constant density (0.735 g/mL).

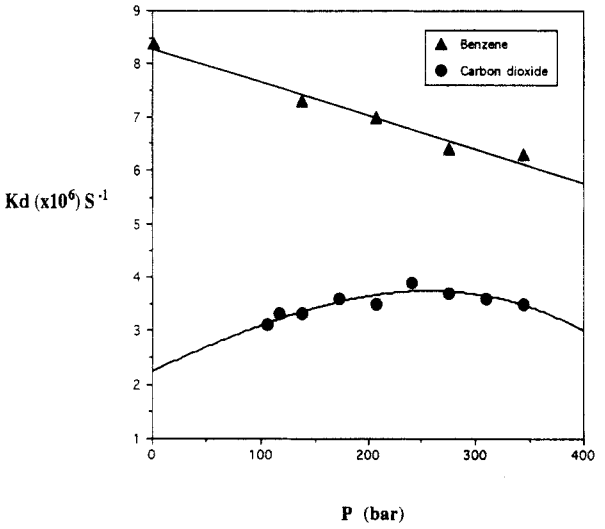

Figure 5. Dependence of the decomposition rate of AIBN in benzene and in supercritical CO_2 as a function of pressure at constant temperature 59.4 (±0.1) °C.

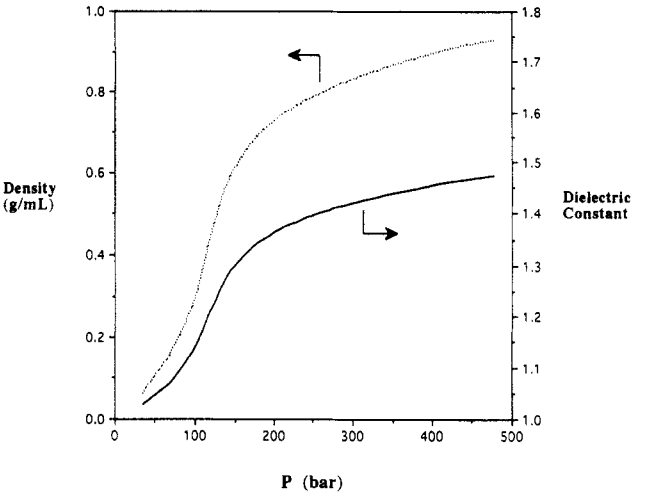

Figure 6. Dependence of CO_2 density and dielectric strength on pressure at 59.4 (±0.1) °C.

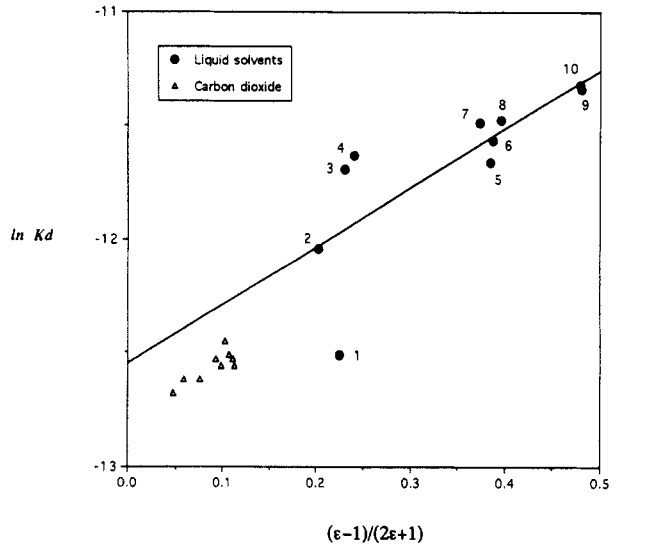

Figure 7. Kirkwood correlation for the decomposition rate of AIBN at 59.4 (±0.1) °C in liquid organic solvents: (1) carbon tetrachloride; (2) cyclohexane; (3) benzene; (4) toluene; (5) ethyl acetate; (6) acetic acid; (7) bromobenzene; (8) aniline; (9) dimethylformamide; (10) nitrobenzene. Points 2, 3, 4, and 7 are from ref 38 and all others are from ref 35. All rate constants at temperatures other than 59.4 °C are converted to the value at 59.4 °C using the Arrhenius equation (activation energy data from ref 35). The open symbols represent the results obtained in supercritical CO_2. The line was calculated using only the data measured in liquid organic solvents at atmospheric pressure.

measured in CO_2 are lower than the decomposition rates measured in benzene at the same pressure and temperature. Moreover, a maximum is observed for the measured decomposition rate in CO_2 as a function of pressure. The following discussion will first focus on why the decomposition rates of AIBN are lower in CO_2 than in benzene and then we will address the maximum in the decomposition rate observed in CO_2 as a function of pressure.

To rationalize the lower decomposition rates of AIBN in CO_2 versus benzene, one must first consider the density and dielectric strength of CO_2 and benzene. Due to the high compressibility of a supercritical fluid, the density and dielectric constant changes dramatically near the critical point. The densities and dielectric constants of CO_2 at 59.4 °C can be calculated using the NIST equation of state[36] and Kirkwood–Frohlich equation,[37] respectively, and are shown in Figure 6 as a function of pressure. In Figure 7, $\ln(k_d)$ for the thermal decomposition of AIBN in conventional liquid solvents as well as in supercritical CO_2 are plotted versus the Kirkwood parameter $(\epsilon - 1)/(2\epsilon + 1)$.[39] The line drawn represents a linear least squares fit of only the previously reported data for reactions in *liquid* organic solvents. The correlation shows the decomposition rate of AIBN increases with increasing solvent polarity, indicating that a dipolar interaction between the reactant's transition state and the solvent medium exists. Relative to ionic reactions, where solvent effects manifest themselves in reaction rates that span several orders of magnitude, radical reactions are not very solvent sensitive with rates that usually span less than an order of magnitude.[40] The decomposition rate of AIBN measured by others in various liquid solvents also shows a solvent dependence with an overall variation in the rate constant of a factor of 2–4.[41–43] The difference in the rate constants measured in CO_2 and in benzene reported herein falls within this range as well and their relative magnitudes are in the correct regime as indicated by the correlation with the Kirkwood parameter (Figure 7). Hence, the lower decomposition rate in CO_2 is attributable to the lower dielectric constant of supercritical CO_2 relative to benzene. This is further supported by the enhanced decomposition rate measured in CO_2 upon addition of THF, a polar cosolvent (see Figure 3).

If we assume a dipolar interaction exists between solvent and the transition state during the thermal decomposition

of AIBN, applying Kirkwood's formula to transition state theory we obtain an expression for the rate constant:[40]

$$\ln k_d^\circ = \ln k_0 - \left(\frac{N_A}{RT}\right)\left(\frac{\epsilon - 1}{2\epsilon + 1}\right)\left(\frac{\mu_A^2}{r_A^3} - \frac{\mu_\ddagger^2}{r_\ddagger^3}\right) \quad (2)$$

Where k_d° represents the rate constant without consideration of an intrinsic activation volume effect, k_0 is the rate constant in a medium of unity dielectric constant, N_A is Avogadro's constant, μ_A and $\mu_\ddagger$ are the dipole moments of AIBN and its transition state, respectively, and r_A and $r_\ddagger$ are molecular radii of AIBN and its transition state, respectively. In this study, the trans configuration of AIBN is used and it is a reasonable assumption that it has no dipole moment ($\mu_A = 0$) which reduces eq 2 to:

$$\ln k_d^\circ = \ln k_0 + \left(\frac{N_A}{RT}\right)\left(\frac{\epsilon - 1}{2\epsilon + 1}\right)\left(\frac{\mu_\ddagger^2}{r_\ddagger^3}\right) \quad (3)$$

The exact nature of the dipole moment that develops during the transition state during the thermal decomposition of AIBN is unclear. Some authors[43,44] have proposed that the initial thermolysis of the azo linkage occurs in two stages and, in particular, the diazenyl radical has been suggested to have transient existence at −196 °C.[45] Another possibility is that *trans*-AIBN undergoes isomerization to the cis isomer which results in a more cis-like transition state which has a higher dipole moment.[23] Regardless, a good correlation between ln k_d and the Kirkwood parameter does indeed exist and is indicative of a dipolar stabilization of the transition state by the solvent.

According to transition state theory, for a simple unimolecular reaction, the pressure effect on the rate constant can be expressed as

$$\Delta V^\ddagger = -RT\left(\frac{\delta \ln k_c}{\delta P}\right)_T = V^\ddagger_A - V_A + \sum \nu_i RT\kappa \quad (4)$$

where $\Delta V^\ddagger$ is the activation volume, $V_A^\ddagger$ and V_A are the partial molar volume of the transition state and the reactant, respectively, k_c is the rate constant, and κ is the compressibility of the solvent.[46] Normally, three factors determine the partial molar volume of a dissolved species in solution: (i) the intrinsic size of the reacting species as determined by its van der Waals radius; (ii) the interaction of the species with the solvent to cause electrostriction; (iii) the interaction of the species with all the solute species, including itself.[47] For dilute solution, (iii) is negligible and to a first approximation the observed activation volume can be regarded as the sum of an intrinsic and a solvational component as[46]

$$\Delta V^\ddagger = \Delta V^\ddagger_{\text{solvation}} + \Delta V^\ddagger_{\text{intrinsic}} \quad (5)$$

The intrinsic activation volume results from the reorganization of the reacting species, i.e., changes in bond lengths and angles during the formation of the transition state, and is generally considered to be independent of solvent. The solvation activation volume represents all volume changes associated with changes in polarity, electrostriction, and dipole interactions during the course of the reaction. The literature value of $\Delta V^\ddagger_{\text{intr}}$ for the thermal decomposition of AIBN is ca. +13.1 mL/mol[35] and the value of $\Delta V^\ddagger_{\text{intr}}$ in benzene from our results is +23.6 mL/mol, which is considerably higher than reported values. However, according to Ewald[48] the depression of the decomposition rate with pressure is more pronounced at lower pressures (i.e., 0–1000 atom), leading to an overestimate of the intrinsic activation volume for the range of pressures studied in this work.

Using a linear least squares treatment, we can obtain an expression for the decomposition rate as a function of the solvent dielectric constant from the Kirkwood correlation plot for the thermal decomposition rate of AIBN in liquid organic solvents (Figure 7):

$$\ln k_d^\circ = -a + b\left(\frac{\epsilon - 1}{2\epsilon + 1}\right) \quad (6)$$

To account for the intrinsic activation volume effect on the thermal decomposition of AIBN, we begin with the definition of the intrinsic activation volume:

$$\left(\frac{\delta \ln k_d'}{\delta P}\right)_T = \frac{-\Delta V^\ddagger_{\text{intr}}}{RT} \quad (7)$$

where k_d' represents the rate constant after accounting for solvation effects.[49] Upon integration of eq 7 we obtain

$$\ln k_d = \ln k_d^\circ - \left(\frac{\Delta V^\ddagger_{\text{intr}}}{RT}\right)P \quad (8)$$

Combining with eq 6 gives

$$\ln k_d = -a + b\left(\frac{\epsilon - 1}{2\epsilon + 1}\right) - \left(\frac{\Delta V^\ddagger_{\text{intr}}}{RT}\right)P \quad (9)$$

This equation can be further reduced since the dielectric functional $\epsilon(P)$ of the pressure can be easily calculated as described earlier (Figure 7). Hence, the rate constants can simply be calculated as a function of pressure:

$$\ln k_d = -a + b\left(\frac{\epsilon(P) - 1}{2\epsilon(P) + 1}\right) - \left(\frac{\Delta V^\ddagger_{\text{intr}}}{RT}\right)P \quad (10)$$

Figure 8A shows a series of calculated rate constant (eq 10 with $a = 12.55$ and $b = 2.58$) as a function of pressure in CO_2 for various intrinsic activation volumes ranging from +13.1 to +40 mL/mol along with the experimentally determined rate constants in benzene and in CO_2. It is obvious that the calculated rate constants also go through a maximum and a good correlation exists for $\Delta V^\ddagger_{\text{intr}}$ = +23.6 mL/mol at high pressures; however, at low pressures the rate constants are overestimated, which predicts the theoretical maximum to be at a lower pressure than the experimental results indicate.

The expression for the line obtained from the Kirkwood plot (eq 6 and Figure 7) did not take into account any of the rate constants measured in CO_2 and only used the rates measured in *liquid* solvents because we wanted to completely isolate the effect of pressure versus solvent dielectric strength. Unfortunately, however, there is no conventional liquid organic solvent with a dielectric constant as low as that for supercritical CO_2, and therefore eq 10 with $a = 12.55$ and $b = 2.58$ is not optimized for solvents with low dielectric strengths as illustrated by the poor correlation of the calculated rate constants with the experimentally measured values at low pressures. Because of this limitation, we can reevaluate the Kirkwood relationship by considering the rate constant measured in CO_2 at the lowest pressure which modifies the slope and intercept of eq 6. By choosing the rate measured at the lowest pressure, we minimize the influence of pressure on the rate in an effort to separate the dielectric strength effect from the pressure effect for the calculation of rate constants. Considering the rate measured at the lowest CO_2 pressure along with the values reported in conventional liquid solvents, the rate constants can be reevaluated using eq 10 with the new constants $a = 12.69$ and $b = 2.95$. Figure 8B shows the calculated rate constants using the new expression with intrinsic activation volumes reported

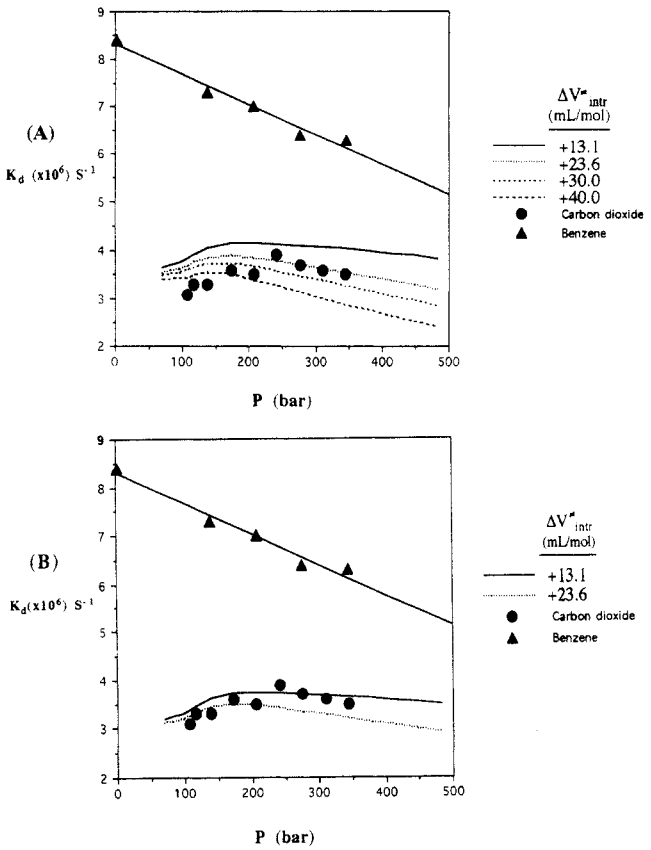

Figure 8. Graph of AIBN decomposition rate constants (k_d) versus pressure (▲) benzene; (●) CO_2). The series of line on the lower portion of the graphs represent the calculated rate constants using (A) eq 10 with a = 12.55 and b = 2.58 and with ΔV^*_{intr} = +13.1, +23.6, +30.0, and +40 mL/mol and (B) eq 10 with a = 12.69 and b = 2.95 and with ΔV^*_{intr} = +13.1 and +23.6 mL/mol.

elsewhere (ΔV^*_{intr} = +13.1 mL/mol) and herein (ΔV^*_{intr} = +23.6 mL/mol). As can be seen, very good correlations now exist for both intrinsic activation volumes using the reevaluated Kirkwood expression. In the lower pressure region (P < 241 bar) the dielectric constant of CO_2 increases with pressure significantly. In this region, the solvational effect dominates and the decomposition rate of AIBN increases with increasing pressure. However, as the pressure is increased even further (P > 241 bar), CO_2 becomes increasingly incompressible—similar to conventional liquid solvents—and hence the change of dielectric solvent strength is small (see Figure 6), which leads to an increasingly insignificant augmentation of the decomposition rate. Because of the relatively small increase in CO_2 solvent strength with pressure in this incompressible region, the intrinsic activation volume effect dominates, which leads to the observed decrease in the rate of decomposition at higher pressures. These two opposing parameters—the solvation effect, which enhances the rate with increasing pressure, and the intrinsic activation volume effect, which decreases the rate with increasing pressure—results in a maximum for the rate constant (Figure 8).

This approach to calculating rate constants for reactions in supercritical fluids based on Kirkwood correlations and intrinsic activation volumes obtained in conventional liquid solvents should also be applicable to other reactions as well. In fact, this approach predicts that it should also be possible to observe a minimum in a rate constant as a function of pressure. This would occur for a reaction conducted in an inert supercritical fluid that has a negative intrinsic activation volume and transition state that has a smaller dipole moment associated with it relative to the ground state.

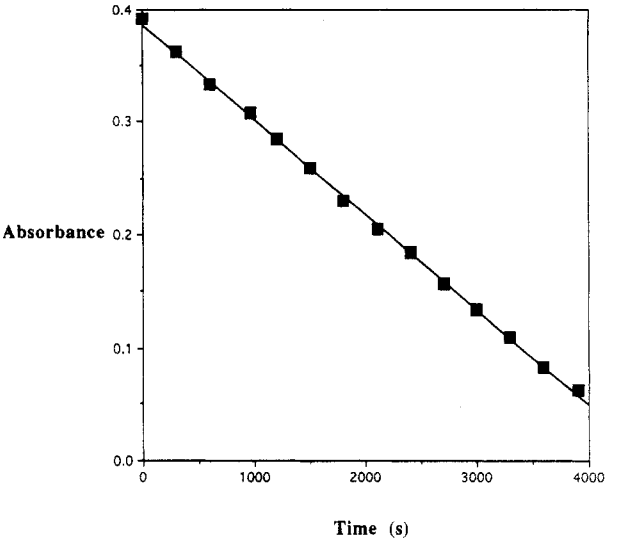

Figure 9. Absorption of galvinoxyl (762 nm) with time in supercritical CO_2 solution of AIBN; T = 59.4 (±0.1) °C, P = 276 (±0.5) bar, [AIBN] = 6.1 × 10^{-3} M, [galvinoxyl] = 4.74 × 10^{-4} M.

Initiation Efficiency. As reported by Bartlett,[50] galvinoxyl is a good radical scavenger and is generally considered superior to 2,2-diphenylpicrylhydrazyl (DPPH) or iodine since it reacts quantitatively with either carbon or oxygen-centered free radicals. In this study, galvinoxyl was used as the radical scavenger to measure the initiation efficiency of AIBN in supercritical CO_2. By following the decreasing absorbance of galvinoxyl at 762 nm with time and plotting the results according to[51]

$$A_t = A_0 - (2fk_d[I]_0\epsilon l)t \qquad (11)$$

where t = time, A_0 and A_t are the absorbance of galvinoxyl at time = 0 and time = t, respectively, $[I]_0$ is the initial initiator concentration, ϵ is the extinction coefficient of galvinoxyl, and l is the path length of the high-pressure cell, the initiator efficiency can be measured. As shown in Figure 9, a straight line is obtained for carbon dioxide at 59.4 (±0.1) °C and 276 (±0.5) bar, and from the slope the efficiency factor f = 0.83 (±0.02) was calculated. This high value can be contrasted with the efficiency factor of AIBN measured in benzene, which is only 0.53 (±0.02) at 59.4 (±0.1) °C. The high radical efficiency measured in supercritical carbon dioxide is presumably the result of the low viscosity of CO_2 at these conditions[52] compared to that of benzene. The viscosity of benzene at 60 °C is 3.95 × 10^{-3} P;[53] however, the viscosity of supercritical CO_2 at 207 bar (ρ = 0.738 g/mL) at the same temperature is only ca. 6.0 × 10^{-4} P.[54] This amounts to supercritical CO_2 having about 1 order of magnitude lower viscosity than benzene.

The initiation efficiencies of AIBN in supercritical CO_2 at different pressures were also measured. For the range of pressures studied (138–345 bar), the initiation efficiency is always higher in CO_2 than it is in benzene and there is no significant variation in initiation efficiency with pressure. The invariant nature of initiation efficiency as a function of pressure is probably the result of the insignificant viscosity change for supercritical CO_2 in this pressure range.

Conclusions

The thermal decomposition of AIBN in supercritical carbon dioxide was investigated to probe the influence of

the tunability of solvation on polymerization kinetics. Decomposition product analysis indicates that supercritical carbon dioxide is effectively inert to the free radical reactions. Investigation of the pressure effects on the decomposition rate of AIBN in supercritical CO_2 shows that the reaction rate in supercritical fluids can be adjusted by varying the pressure. Kirkwood solution theory provides a simple but useful method to analyze the change of reaction rate with the pressure. Knowing the changes of the molecular volume ($\Delta V^{\ddagger}_{intr}$) and the dipole moment ($\Delta\mu^{\ddagger}$) during the reaction going from the reactants toward the transition state, we can discern the solvation effect on the kinetics from the intrinsic activation effect. By combining and correlating these two effects, the overall pressure effect can be estimated. This approach may be applicable to other types of reactions in supercritical fluids and may aid in predicting the optimum reaction conditions of various reactions in supercritical fluids. For reactions in which the solvation effect plays a more significant role (such as anionic reactions), the pressure effects will be more dramatic and the significance of this kind of theoretical analysis will be more obvious. The kinetic information we obtained for the free radical initiation reaction in supercritical CO_2 will facilitate our further investigation of polymerization kinetics in supercritical fluids.

Acknowledgment. We gratefully acknowledge financial support from the DuPont Co., 3M, Unilever Research, the Petroleum Research Fund, and the National Science Foundation Young Investigator Program (J.M.D.). We also thank Professor E. T. Samulski for clarifying discussions.

Supplementary Material Available: FTIR and ^1H and ^{13}C NMR spectra of the reaction mixture for thermal decomposition of AIBN in SCF CO_2 and FTIR and ^1H NMR spectra of the reaction mixture for thermal decomposition of AIBN in THF (4 pages). Ordering information is given on any current masthead page.

References and Notes

(1) DeSimone, J. M.; Guan, Zhibin; Elsbernd, C. S. *Science* **1992**, *257*, 945.
(2) Solomon, S.; Garcia, R. R.; Sherwood, F.; Wuebbles, D. J. *Nature* **1986**, *321*, 755.
(3) (a) Paulaitis, M. E.; Krukonis, K. J.; Kurnik, R. T.; Reid, R. C. *Rev. Chem. Eng.* **1983**, *1*(2), 179. (b) Moore, J. W.; Pearson, R. G. *Kinetics and Mechanism*, 3rd ed.; John Wiley & Sons: New York, 1981.
(4) McHugh, M.; Krukonis, V. *Supercritical Fluid Extraction—Principles and Practice*; Butterworths: Boston, 1986.
(5) Elsbernd, C. S.; DeSimone, J. M.; Hellstern, A. M.; Smith, S. D.; Gallagher, P. M.; Krukonis, V. J.; McGrath, J. E. *Polym. Prepr. (Am. Chem. Soc., Div. Polym. Chem.)* **1990**, *31*(1), 673.
(6) DeSimone, J. M.; Hellstern, A. M.; Ward, T. C.; McGrath, J. E.; Smith, S. D.; Gallagher, P. M.; Krukonis, V. J.; Stejskal, J.; Strakova, D.; Kratochvil, P. *Multiphase Macromolecular Systems*; Culbertson, W., Ed.; *ACS: Washington, DC*, 1989.
(7) DeSimone, J. M.; Hellstern, A. M.; Ward, T. C.; McGrath, J. E.; Smith, S. D.; Gallagher, P. M.; Krukonis, V. J.; Stejskal, J.; Strakova, D.; Kratochvil, P. *Polym. Prepr. (Am. Chem. Soc., Div. Polym. Chem.)* **1988**, *29*(2), 116.
(8) DeSimone, J. M.; Smith, S. D.; Hellstern, A. M.; Ward, T. C.; McGrath, J. E.; Gallagher, P. M.; Krukonis, V. J. *Polym. Prepr. (Am. Chem. Soc., Div. Polym. Chem.)* **1988**, *29*(1), 361.
(9) Elsbernd, C. S.; Mohanty, D. K.; McGrath, J. E.; Gallagher, P. M.; Krukonis, V. J. *Polym. Prepr. (Am. Chem. Soc., Div. Polym. Chem.)* **1987**, *28*(2), 399.
(10) Kumar, S. K.; Suter, U. W.; Reid, R. C. *Fluid Phase Equilib.* **1986**, *29*, 373.
(11) Meilchen, M. A.; Kulikowski, K. J.; McHugh, M. A. *Polym. Prepr. (Am. Chem. Soc., Div. Polym. Chem.)* **1990**, *31*(1), 671.
(12) Subramaniam, B.; McHugh, M. A. *Ind. Eng. Chem. Process Des. Dev.* **1986**, *25*, 1.
(13) Ehrlich, P. *Adv. Polym. Sci.* **1970**, *7*, 386 and references therein.
(14) Ehrlich, P. *J. Polym. Sci., Part A* **1965**, *3*, 131.
(15) Kumar, S. K.; Reid, R. C.; Suter, U. W. *Polym. Prepr. (Am. Chem. Soc., Div. Polym. Chem.)* **1986**, *27*(2), 224.
(16) Kumar, S.; Suter, U. *Polym. Prepr. (Am. Chem. Soc., Div. Polym. Chem.)* **1987**, *28*(2), 286.
(17) Sarai, V. P.; Kiran, E. *Polym. Prepr. (Am. Chem. Soc., Div. Polym. Chem.)* **1990**, *31*(1), 687.
(18) Varadarajan, G. S. Ph.D Dissertation, Massachusetts Institute of Technology, 1990.
(19) Moore, P. W.; Ayscough, F. W.; Clouston, J. G. *J. Polym. Sci., Polym. Chem. Ed.* **1977**, *15*, 1291.
(20) Asano, T.; Le Noble, W. J. *Chem. Rev.* **1978**, *78*, 407.
(21) Odian, G. *Principles of Polymerization*, 2nd ed.; John Wiley & Sons: New York, 1981; Chapter 3.
(22) Hammond, G. S.; Trapp, O. D.; Keys, R. T.; Neff, D. L. *J. Am. Chem. Soc.* **1959**, *81*, 4878.
(23) Hammond, G. S.; Sen, J. N.; Boozer, C. E. *J. Am. Chem. Soc.* **1955**, *77*, 3244.
(24) Talat-Erben, M.; Bywater, S. *J. Am. Chem. Soc.* **1955**, *77*, 3710.
(25) Osugi, J.; Sata, M.; Sasaki, M. *Rev. Phys. Chem. Jpn.* **1963**, *33*(2), 53.
(26) Wu, Chin-Hua S.; Hammond, G. S.; Wright, J. M. *J. Am. Chem. Soc.* **1960**, *82*, 5386.
(27) Kim, S.; Johnston, K. P. *Ind. Eng. Chem. Res.* **1987**, *26*, 1206.
(28) Kim, S.; Johnston, K. P. *AIChE J.* **1987**, *33*, 1603.
(29) Freed, B. K.; Biesecker, J.; Middleton, W. J. *J. Fluor. Chem.* **1990**, *48*, 63.
(30) Lemert, R. M.; DeSimone, J. M. *J. Supercrit. Fluids* **1991**, *4*, 186.
(31) Debenedetti, P. G. *Chem. Eng. Sci.* **1987**, *42*, 2203.
(32) ^1H NMR, ^{13}C NMR, and FTIR spectra for AIBN thermal decomposition products in supercritical CO_2 are provided as supplementary material.
(33) Forbes, M. D. E.; Peterson, J.; Breivogel, C. S. *Rev. Sci. Instrum.* **1991**, *62*, 2662. Forbes, M. D. E. *Rev. Sci. Instrum.* **1993**, *64*, 379.
(34) Hammond, G. S.; Wu, C. S.; Trapp, O. D.; Warkentin, J.; Keys, R. T. *J. Am. Chem. Soc.* **1960**, *82*, 5394.
(35) Brandrup, J.; Immergut, H. *Polymer Handbook*, 2nd ed.; Wiley: New York, 1975.
(36) Ely, J. F. *CO_2PAC: A Computer Program to Calculate Physical Properties of Pure CO_2*, National Bureau of Standards, Boulder, CO, 1986.
(37) Smyth, C. P. *Dielectric Behavior and Structure*; McGraw-Hill: New York, 1955.
(38) Henrici-Olive, V. G.; Olive, S. *Makromol. Chem.* **1962**, *58*, 188.
(39) Abraham, M. H.; Grallier, P. L. *J. Chem. Soc., Perkin Trans. 2*, **1976**, 1735.
(40) Reichardt, C. *Solvent Effects in Organic Chemistry*, 2nd ed.; Verlag Chemie: Weinheim, New York, 1979; Chapter 5.
(41) Denisov, E. T. *Liquid-Phase Reaction Rate Constants*; IFI/Plenum Data Co.: New York, Washington, London, 1974.
(42) Moroni, A. F. *Makromol. Chem.* **1967**, *105*, 43.
(43) Yamamoto, O.; Yamashita, J.; Hashimoto, H. *Kogyo Kagaku Zasshi* **1968**, *71*, 223; *Chem. Abstr.* **1968**, *69*, 66644u.
(44) Engel, P. S. *Chem. Rev.* **1980**, *80*, 99.
(45) Ayscough, P. B.; Brooks, B. R.; Evans, H. E. *J. Phys. Chem.* **1964**, *68*, 3889.
(46) Eldik, R. V.; Asano, T.; Le Noble, W. J. *Chem. Rev.* **1989**, *89*, 549.
(47) Hamann, S. D. *Rev. Phys. Chem. Jpn.* **1980**, *50*, 147.
(48) Ewald, A. H. *Discuss. Faraday Soc.* **1956**, *22*, 138.
(49) The term accounting for the solvent compressibility is not included despite the use of pressure-dependent concentration units (i.e., moles/liter) in the rate expression because the sum of the stoichiometric coefficients for this reaction equals zero and therefore the compressibility term can be neglected.[46]
(50) Bartlett, P. D.; Funahashi, T. *J. Am. Chem. Soc.* **1962**, *84*, 2596.
(51) Areizaga, J. F.; Guzman, G. M. *Makromol. Chem., Macromol. Symp.* **1988**, *20/21*, 77.
(52) O'Shea, K. E.; Combes, J. R.; Fox, M. A.; Johnston, K. P. *Photochem. Photobiol.* **1991**, *54*, 571.
(53) Lide, D. R. *CRC Handbook of Chemistry and Physics*, 73rd ed.; CRC: Boca Raton, FL, 1992–1993. The viscosity of benzene at 60 °C is interpolated from a plot of η versus $1/T$ using an exponential correlation.
(54) Iwasaki, H.; Takahashi, M. *J. Chem. Phys.* **1981**, *74*(3), 1930. The viscosity of CO_2 at 60 °C and 207 bar is estimated to be 6.0×10^{-4} P.